Available online at www.sciencedirect.com
SCIENCE DIRECT®
Biochemical and Biophysical Research Communications 337 (2005) 52–60
BBRC
www.elsevier.com/locate/ybbrc

Nano neodymium oxide induces massive vacuolization and autophagic cell death in non-small cell lung cancer NCI-H460 cells ☆

Yong Chen, Lisong Yang, Chao Feng, Long-Ping Wen *

Hefei National Laboratory for Physical Sciences at Microscale and School of Life Sciences, University of Science and Technology of China, Hefei, Anhui 230027, China

Received 29 August 2005
Available online 15 September 2005

Abstract

Neodymium, a rare earth element, was known to exhibit cytotoxic effects and induce apoptosis in certain cancer cells. Here we show that nano-sized neodymium oxide (Nano Nd_2O_3) induced massive vacuolization and cell death in non-small cell lung cancer NCI-H460 cells at micromolar equivalent concentration range. Cell death elicited by Nano Nd_2O_3 was not due to apoptosis and caspases were not involved. Electron microscopy and acridine orange staining revealed extensive autophagy in the cytoplasm of the cells treated by Nano Nd_2O_3. Autophagy induced by Nano Nd_2O_3 was accompanied by S-phase cell cycle arrest, mild disruption of mitochondrial membrane potential, and inhibition of proteasome activity. Bafilomycin A1, but not 3-MA, induced apoptosis while inhibiting autophagy. Our results revealed a novel biological function for Nano Nd_2O_3 and may have implications for the therapy of non-small cell lung cancer.

Keywords: Nano neodymium oxide; Autophagy; Cell death; Vacuolization

Despite the tremendous amount of work and much progress in the last decades, non-small cell lung cancer (NSCLC) remains one of the most lethal and difficult diseases to treat. The leading treatment regimen, chemotherapy, shows poor response rates in NSCLC patients, with relatively short duration and rare complete remissions [1,2]. There is a great need for the development of new and more potent drugs to conquer NSCLC.

Autophagy, a cellular process for eliminating long-lived proteins and organelle components, has received much attention in the recent years [3,4]. It is characterized by sequestration of bulk cytoplasm and organelles in autophagic vesicles and subsequent delivery to and degradation by the cell's own lysosomal system [5,6]. A role for autophagy in cancer has been implicated in a number of studies. Heterogeneous disruption of the autophagy gene Beclin 1 was shown to increase tumorigenesis in mice [7]. A variety of chemical or physical treatments, including oncogenic Ras [8], radiation [9], arsenic trioxide [10], ceramide [11], temozolomide [12], dopamine [13], endostatin [14], histone deacetylase (HDAC) inhibitors, butyrate and suberoylanilide hydroxamic acid (SAHA) [15], have been reported to induce autophagy in certain cancer cells. Normal cells, unlike the rapidly growing cancer cells, are expected to be less sensitive to pro-autophagic stimuli due to lower metabolic demands and normal activity of regulators such as PI3K and Akt [3]. Thus, finding potent autophagy-inducing agents may be of value for cancer therapy.

Several rare earth elements, including neodymium, have been reported to be cytotoxic to cancer cells [16,17]. The documented effects included suppression of cell growth and induction of apoptosis [17,18]. However, there has been no published report concerning the effect of rare earth

☆ *Abbreviations:* NSCLC, non-small cell lung cancer; Nano Nd_2O_3, nano-sized neodymium oxide; 3-MA, 3-methyladenine; TRAIL, TNF-related apoptosis-inducing ligand; PI, propidium iodide; Z-VAD-FMK, arbobenzoxy-Val-Ala-Asp-fluoromethyl ketone; FACS, fluorescence activated cell sorting; AVO, acidic vesicular organelle; TEM, transmission electron microscopy.

* Corresponding author. Fax: +86 551 3600426.
E-mail address: lpwen@ustc.edu.cn (L.-P. Wen).

0006-291X/$ - see front matter © 2005 Elsevier Inc. All rights reserved.
doi:10.1016/j.bbrc.2005.09.018

elements on autophagy. Here we show that nano-sized neodymium oxide (Nano Nd_2O_3) induced massive vacuolization and autophagic cell death in non-small cell lung cancer NCI-H460 cells in the micromolar equivalent concentration range.

Materials and methods

Reagents. Nano Nd_2O_3 (mean diameter 80 nm) and nano cerium oxide (mean diameter 80 nm) were from Fangyuan Nanomaterial Research Institute (China). Neodymium chloride, trypan blue, propidium iodide, rhodamine 123, acridine orange, and SucLLVY-AMC were purchased from Sigma (USA). TRAIL was from Calbiochem (USA). Caspase family inhibitor Z-VAD-FMK was from Biovision (USA). Bafilomycin A1 was purchased from Wako Pure Chemical Industries (Japan). 3-MA (Wako, Japan) was a kind gift from Professor Yoshihide Tsujimoto (Osaka University, Graduate School of Medicine). Reagents were dissolved in PBS, distilled water or DMSO according to manufacturer's instructions. 3-MA was dissolved in PBS at 10 mg/ml and heated to yield a clear, colorless solution before use. Annexin V-FITC apoptosis detection kit was purchased from Beijing Biosea Biotechnology (China). Caspase 3/9 spectrometric detection kits were from Nanjin Keygen Biotech (China).

Cell line. Human NCI-H460 cell line was purchased from Type Culture Collection of Chinese Academy of Sciences (Shanghai, China). Cells were cultured in RPMI 1640 (Invitrogen, USA) supplemented with 10% fetal bovine serum (Invitrogen), 100 U/ml penicillin, and 100 μg/ml streptomycin.

Trypan blue viability assay. After trypsinization, cells were suspended in PBS and mixed with an equal volume of 0.4% trypan blue in PBS. The percentage of stained cells was determined by using a hemocytometer. At least 150 cells were scored, with each sample repeated three times.

Cell cycle analysis. After trypsinization, cells were permeabilized by 70% ethanol, incubated with propidium iodide and RNase A, and analyzed for DNA content by FACSCalibur (Becton–Dickinson, USA). Data were analyzed by ModFit 3.1 (Verity Software House, USA).

Apoptosis assay by annexin V staining. Cells (5×10^5) were harvested by trypsinization and washed twice with PBS. Washed cells were resuspended in 200 μl binding buffer (PBS containing 1 mM calcium chloride). FITC-conjugated annexin V (0.5 μg/ml final concentration) was added according to the manufacturer's instructions (Biosea, China). After incubation for 20 min at room temperature, 400 μl binding buffer was added, and samples were immediately analyzed on a FACSCalibur flow cytometer (Becton–Dickinson) with excitation using a 488 nm argon ion laser.

Apoptosis detection by Hoechst dye staining. Cells were cultured in 24-well plates. After treatment, the culture medium was removed and 1 ml of pre-warmed Hoechst 33342 dye solution (1 μg/ml) was added to every well. After incubation at 37 °C for 10 min, the solution was replaced by 1 ml pre-warmed PBS and cells were examined under a fluorescent microscope (Olympus, Japan). Three sections were selected and examined randomly for every sample (at least 350 cells). Cells with condensed nuclei (apoptotic) were counted and the percentage of apoptotic cells was calculated.

Autophagy assay by quantification of AVOs. Cells were trypsinized, collected, and stained with acridine orange (final concentration: 0.5 μg/ml) for 10 min. After centrifugation, cells were resuspended in PBS and analyzed with FACSCalibur (Becton–Dickinson). Data were analyzed using FCS Express V2 (De Novo Software, USA).

Transmission electron microscopy. Cells were harvested by trypsinization, washed twice with PBS, and fixed with 2% paraformaldehyde/2% glutaraldehyde in 0.1 M phosphate buffer (pH 7.4), followed by 1% OsO_4. After dehydration, thin sections were stained with uranyl acetate and lead citrate for observation under a JEOL TEM-100SX electron microscope (JEOL, Japan).

Caspase inhibition assay. NCI-H460 cells were seeded in a 24-well plate and incubated overnight at 37 °C. One hour before treatment with Nano Nd_2O_3 (40 μg/ml) or TRAIL (20 ng/ml), 50μM Z-VAD-FMK (solubilized in DMSO) was added. After 3 days, cell viability was determined by trypan blue staining.

Analysis of mitochondrial membrane potential. Rhodamine 123, a cationic voltage-sensitive probe, was used to detect changes in mitochondrial membrane potential by using flow cytometry. Cells were collected with trypsinization, washed twice with PBS, and stained with 1 μM rhodamine 123 in PBS in the dark at 37 °C for 1 h. Samples were washed, resuspended with PBS, and then analyzed with FACSCalibur (Becton–Dickinson). Data were analyzed using FCS Express V2 (De Novo Software).

Caspase activity assay. To detect caspase activity, we performed spectrometric detection according to manufacturer's instructions. Briefly, 3×10^6 cells were collected and lysed in the lysis buffer. After removal of cell debris, the concentration of proteins in the supernatant (cell extract) was quantified using the Bradford method. Cell extract containing 200 μg protein was incubated with caspase-3 substrate (Ac-DEVD-pNA) or caspase-9 substrate (Ac-LEHD-pNA) at 37 °C in the dark for 4 h. Absorbance at 405 nm was read using a microplate reader. After subtracting the background, the activity of caspases was calculated as OD treated/OD control.

Proteasome activity detection. 20S proteasome activity was assessed as previously described [19,20] with slight modifications. Briefly, cell extract containing 50 μg protein was diluted to 500 μl with SDS buffer [20 mM Hepes (pH 7.8), 0.5 mM EDTA, and 0.03% SDS]. Fluorogenic proteasome substrate Suc-LLVY-AMC (chymotrypsin-like; Sigma) was dissolved in DMSO and added to a final concentration of 80 μM (in 0.8% DMSO). After incubation at 37 °C in the dark for 1 h, substrate hydrolysis was measured by monitoring the release of the fluorescent group AMC using a spectrofluorometer (excitation at 380 nm, emission at 460 nm).

Statistical analysis. All of the experiments were repeated at least three times. The data were expressed as means ± SD. Statistical analysis was performed by using two-tailed Student's t test. The criterion for statistical significance was taken as $p < 0.05$.

Results

Nano Nd_2O_3 caused massive vacuolization in NCI-H460 cells

To assess the effect of Nano Nd_2O_3 on NCI-H460 cells, we added Nano Nd_2O_3 (45 μg/ml, equivalent of 133.8 μM) to the cell culture medium and observed cell morphology under a light microscope. Massive vacuolization in the cytoplasm was seen 2 days after the Nano Nd_2O_3 treatment (Fig. 1A). Vacuoles started to be visible approximately 3.5 h after the addition of Nano Nd_2O_3, and as time progressed, vacuoles became larger and denser (number of vacuoles within a cell increased). Meanwhile, the percentage of cells with at least one visible vacuole also increased with time, and by 48 h over 70% of cells were vacuolated (Fig. 1B). Neodymium chloride, a soluble neodymium compound, and nano-sized cerium oxide, a close neighbor of neodymium oxide in the periodic table, both failed to cause vacuolization in NCI-H460 cell line (data not shown). These results indicated that the ability of Nano Nd_2O_3 to cause cellular vacuolization is both element- and compound-specific.

Nano Nd_2O_3 caused cell death

To assess whether Nano Nd_2O_3 causes cell death, we performed trypan blue viability assay on NCI-H460 cells after treatment with Nano Nd_2O_3 (45 μg/ml). As shown

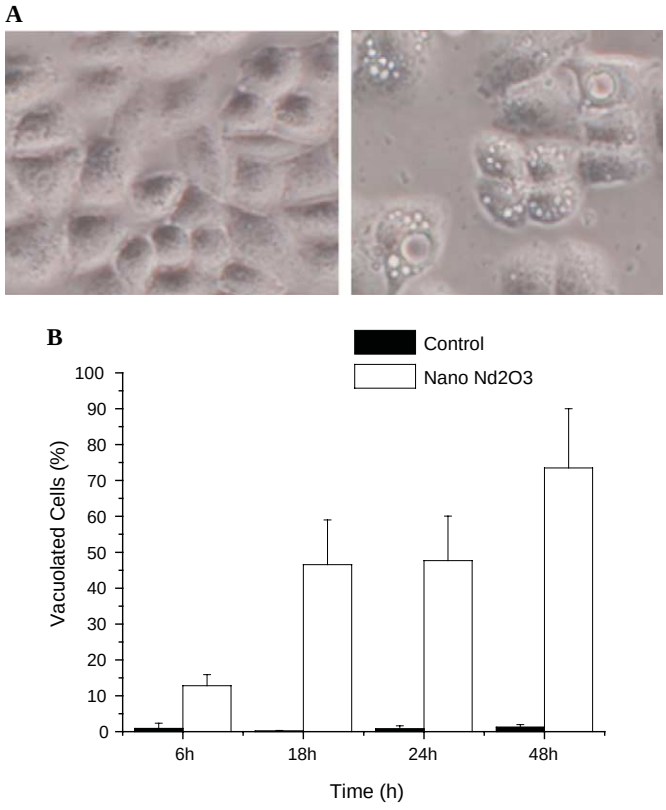

Fig. 1. Massive vacuolization of NCI-H460 cells induced by Nano Nd_2O_3. (A) Direct observation of cells untreated (left panel) or treated with 45 μg/ml of Nano Nd_2O_3 for 48 h (right panel) under a phase contrast microscope (magnification: 200×). (B) Quantification of vacuolization. At least 500 cells from untreated (control) or Nano Nd_2O_{3-} treated (45 μg/ml, 48 h) sample were examined under a light microscope and the percentage of vacuolated cells was calculated. Means ± SD ($n = 3$).

in Fig. 2A, the proportion of dead cells increased dramatically after 3 days of treatment, and after 5 days essentially all cells were dead. In contrast, the proportion of dead cells in the untreated cells remains relatively unchanged throughout the experiment. The effect of Nano Nd_2O_3 to cause cell death is dose-dependent, with the minimum effective dose at 22.5 μg/ml and the maximum effect observed at 225 μg/ml (Fig. 2B).

To confirm loss of viability, we stained cells with PI and observed the same under a fluorescent microscope. The majority of Nano Nd_2O_3-treated cells were PI-positive, while those of non-treated cells were PI-negative (Fig. 2C). Most of the dead cells were shrunk and rounded-up (Fig. 2C), a morphology that is quite different from that observed under necrosis.

Nano Nd_2O_3 induced S-phase cell cycle arrest

To assess whether Nano Nd_2O_3 affects cell cycle, we performed DNA flow cytometric analysis. Three days after treatment of Nano Nd_2O_3 (45 μg/ml) in NCI-H460 cells, the cell population in the S-phase increased from 34.01% to 43.26% while the G1- and G2/M-phase populations decreased from 65.99% to 56.74% (Table 1).

Apoptosis and caspases were not involved in the death induced by Nano Nd_2O_3

To determine whether the cell death induced by Nano Nd_2O_3 involved apoptosis, we stained NCI-H460 cells with FITC-conjugated annexin V and analyzed with FACS. Similar to the case for the untreated cells, Nano Nd_2O_3 (45 μg/ml, 3 days)-treated cells exhibited very little annexin V staining (Fig. 3A). In contrast, NCI-H460 cells treated with Taxol (10 μg/ml, 24 h), a known apoptosis-inducing agent in this cell line, showed a high degree (>85% of cells) of annexin V staining. These results indicated that the cell death elicited by Nano Nd_2O_3 was non-apoptotic.

To gain insight into the mechanism of Nano Nd_2O_3-induced cell death, we investigated the possible involvement of caspases in this process. We first measured the activity of caspases-9 and -3, which are important initiator and effector caspases, respectively. As Fig. 3B shows, neither caspase-3 nor caspase-9 was activated by Nano Nd_2O_3 (45 μg/ml, 3 days), but both caspases were activated by TRAIL (20 ng/ml, 6 h), in the NCI-H460 cells. We also performed caspase inhibition assay and found that Z-VAD-FMK, a broad inhibitor of caspase family members, did not block Nano Nd_2O_3-induced cell death (Fig. 3C). The same concentration (50 μM) of Z-VAD-FMK completely blocked cell death induced by TRAIL. These results indicated that caspases were not involved in Nano Nd_2O_3-induced cell death.

Nano Nd_2O_3 induced autophagy

To assess whether the cell vacuolization induced by Nano Nd_2O_3 involved autophagy, we examined the cells under an electron microscope. As shown in Figs. 4A–D, the majority of Nano Nd_2O_3-treated NCI-H460 cells, but not control cells, contained a number of autophagic vacuoles, with digested materials or almost intact organelles visible, demonstrating the existence of autophagy. Neither chromatin condensation nor nuclear fragmentation was observed, confirming the absence of apoptotic cell death. Consistent with the vacuolization results obtained under a light microscope, electron microscopy did not reveal any autophagic vacuoles for the cells treated with neodymium chloride and nano cerium oxide (data not shown).

To quantify autophagy, we performed FACS analysis after staining with acridine orange. Autophagy is characterized by AVO development, which can be detected and quantified by vital staining of acridine orange. In acridine orange-stained cells, the cytoplasm and nucleolus fluoresce bright green and dim red, whereas acidic compartments fluoresce bright red. The intensity of the red fluorescence is proportional to the degree of acidity and/or the volume of the cellular acidic compartment [9]. As shown in Fig. 4E, Nano Nd_2O_3 treatment increased the proportion of red fluorescent cells from 0.80% (control) to 68.38%. 3-MA, a well-known specific inhibitor of autophagy, inhibited the AVO

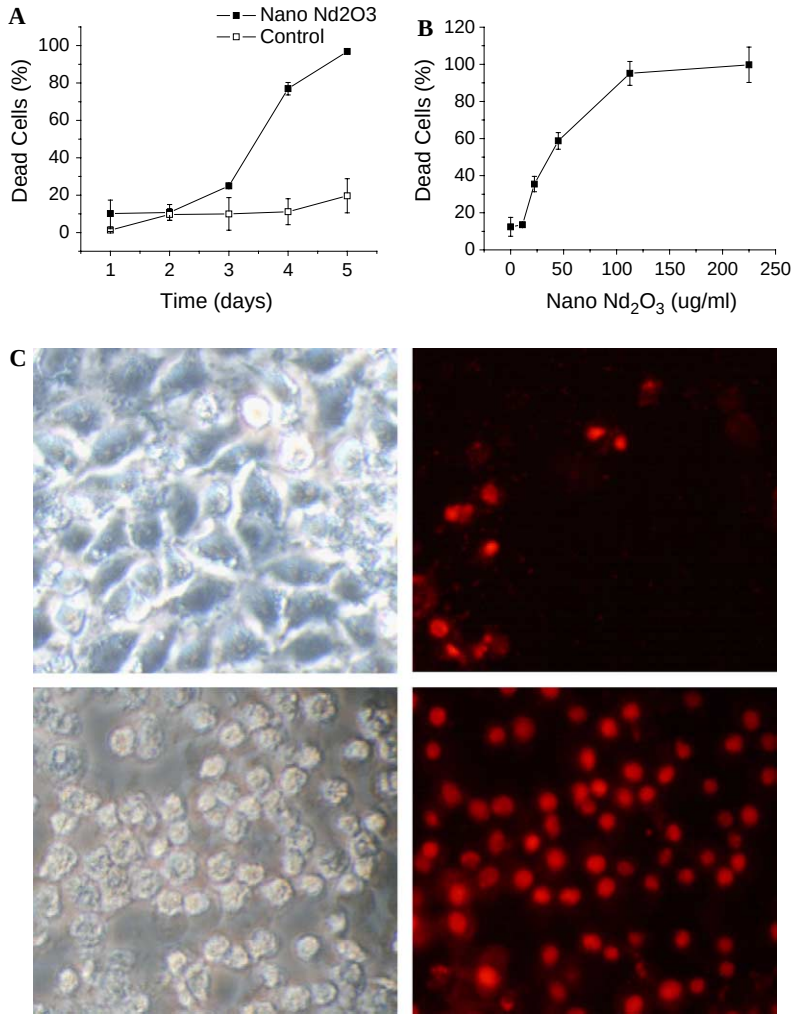

Fig. 2. NCI-H460 cell death induced by Nano Nd_2O_3. (A) Reduced viability after treatment with Nano Nd_2O_3. NCI-H460 cells were treated with 45 μg/ml of Nano Nd_2O_3 or PBS for various times and the percentage of dead cells was assessed by trypan blue staining. Means ± SD ($n = 3$). (B) Dose effect of Nano Nd_2O_3. Cells were treated with 0, 11.25, 22.5, 45, 112.5 or 225 μg/ml of Nano Nd_2O_3 for 4 days and cell viability was assessed by trypan blue staining. Means ± SD ($n = 3$). (C) Confirmation of cell death by PI staining. Untreated cells (upper panel) or cells treated with 45 μg/ml of Nano Nd_2O_3 for 5 days (lower panel) were stained with PI and visualized under light phase contrast microscope (left panel) and fluorescent microscope (right panel). Magnification: 200×.

Table 1
Neodymium oxide induced S-phase arrest

Cell cycle (%)	Control	Neodymium oxide
G1	57.72	48.83
S	34.01	43.26
G2/M	8.26	7.91

NCI-H460 cells were treated with 45 μg/ml of Nano Nd_2O_3 for 24 h. Cells were collected and stained with propidium iodide and analyzed with FACS. The proportion of cells in different phases of the cycle was determined with ModFit LT 3.1 software.

formation caused by Nano Nd_2O_3, as evidenced by a decrease in the proportion of red fluorescent cells from 68.38% (Nano Nd_2O_3 treatment alone) to 30.5% (Nano Nd_2O_3 + 5 mM 3-MA). Bafilomycin A1, another commonly used inhibitor that acts at a late stage of autophagy by inhibiting fusion between autophagosomes and lysosomes, also effectively blocked AVO formation. These data, taken together with the EM, caspase, and annexin V results shown above, supported our conclusion that Nano Nd_2O_3-induced cell death occurs by autophagy, and not apoptosis, in a caspase-independent manner.

Nano Nd_2O_3 decreased the mitochondrial membrane potential

Mitochondria are death signal integrators and play important roles in various death processes. Mitochondria were known to be disrupted during autophagy induced by some agents [10,11], but remained intact in other autophagic cases [21]. To determine the integrity of mitochondria during Nano Nd_2O_3-induced autophagy, we stained NCI-H460 cells after Nano Nd_2O_3 treatment with rhodamine 123, an indicator of mitochondrial membrane poten-

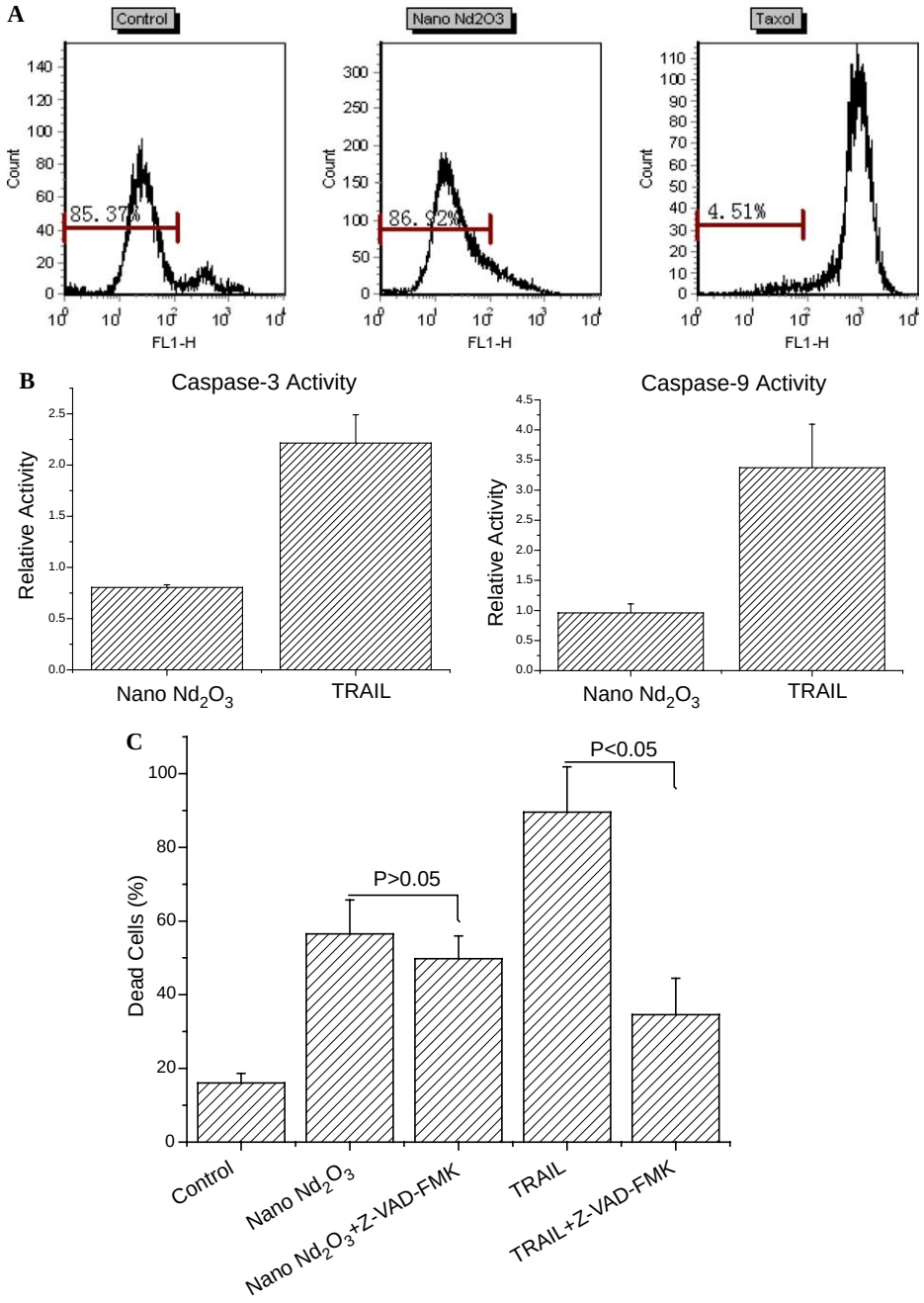

Fig. 3. Cell death induced by Nano Nd_2O_3 in NCI-H460 cells did not involve apoptosis. (A) Quantification of apoptosis. Cells were treated with Nano Nd_2O_3 (45 μg/ml, 3 days) or Taxol (10 μg/ml, 24 h) and assayed for apoptosis by FACS following annexin V-FITC staining. Control cells were treated with PBS. The data shown are representative of three independent experiments. (B) Measurement of caspase activity. Cells were treated with Nano Nd_2O_3 (45 μg/ml, 3 days) or TRAIL (20 ng/ml, 6 h) and assayed for the activity of caspase-3 or caspase-9 by using specific caspase substrates. Control cells were treated with PBS. Results were expressed as the relative activity of treated cells over control cells. (C) Effect of caspase inhibitor. Cells were pre-treated with DMSO or the caspase family inhibitor Z-VAD-FMK (50 μM) for 1 h before treatment with Nano Nd_2O_3 (45 μg/ml, 4 days) or TRAIL (20 ng/ml, 4 days). Control cells were treated with DMSO only. The percentage of dead cells was assessed by trypan blue staining. Means + SD ($n = 3$).

tial and analyzed results by FACS. Nano Nd_2O_3 treatment (45 μg/ml, 3 days) induced mild loss of mitochondria membrane potential, as shown by a modest but significant increase of rhodamine 123-staining cells from 20.67% to 33.33% (Fig. 5). In comparison, H_2O_2, a potent disruptor of mitochondria integrity, caused a complete loss of mitochondrial membrane potential after treatment for 4 h (Fig. 5).

Autophagy induced by Nano Nd_2O_3 is associated with decreased proteasome activity

The proteasome is a large multi-catalytic protease that degrades polyubiquitinated proteins to small peptides. It is composed of two sub-complexes: a catalytic 20S core particle and a regulatory 19S regulatory particle. Degradation by proteasome and autophagy are two important

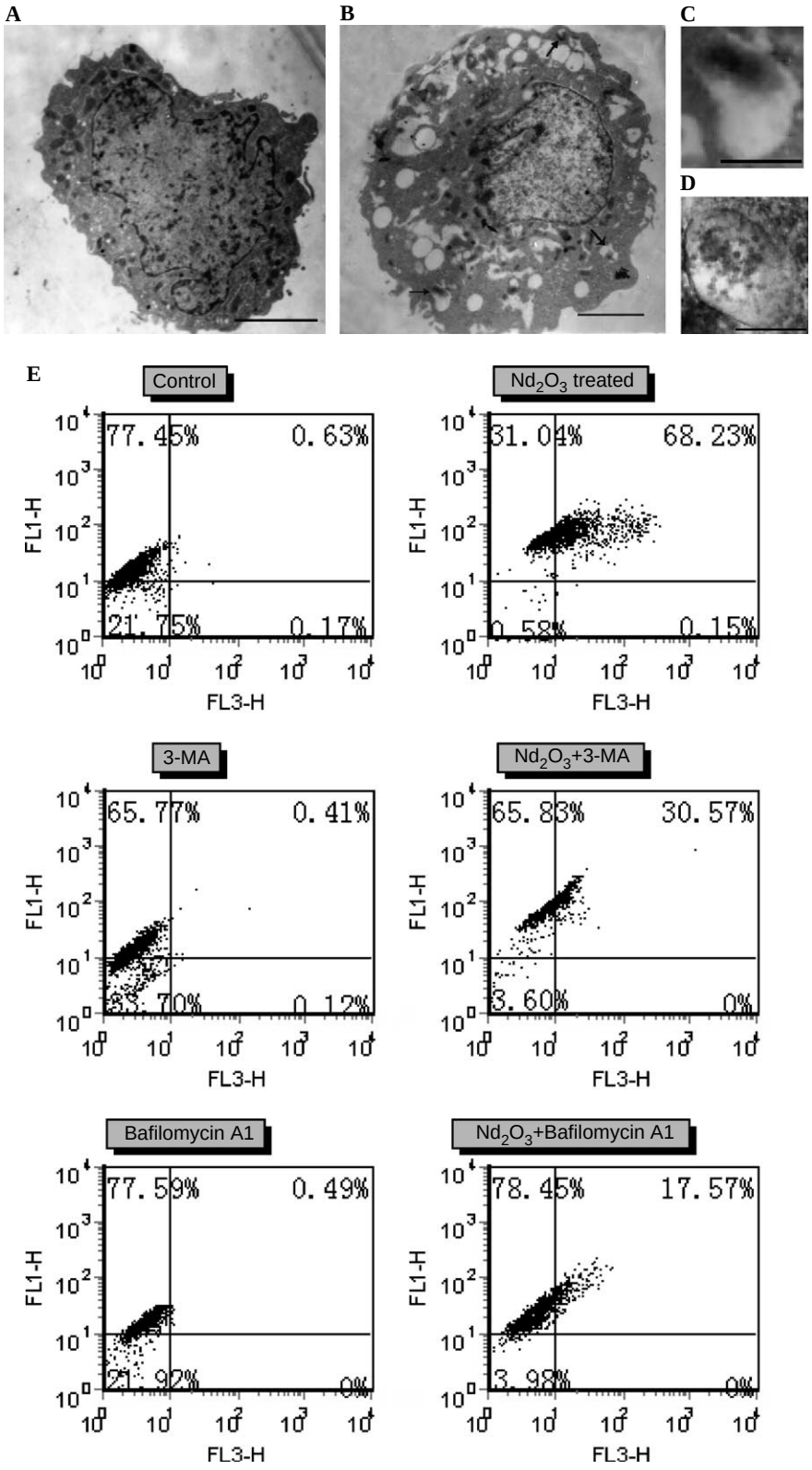

Fig. 4. Induction of autophagy in NCI-H460 cells by Nano Nd_2O_3. (A–D) Ultrastructural features of cells treated with PBS (A) or 45 μg/ml of Nano Nd_2O_3 (B–D) for 2 days, as revealed by TEM. Arrows in (B) indicate representative autophagic vacuoles. (C,D) Autophagic vacuoles containing an almost intact organelle and residual digested material, respectively. Scale bars: 5 μm (A,B); 1 μm (C,D). (E) Quantification of AVOs with acridine orange using FACS scan. Cells were exposed to the supravital stain acridine orange 2 days after treatment with Nano Nd_2O_3 (45 μg/ml), bafilomycin A1 (100 nM) or 3-MA (5 mM). For combination treatments, cells were pre-treated with bafilomycin A1 (100 nM) or 3-MA (5 mM) for 1 h before treatment with Nano Nd_2O_3 (45 μg/ml). Control cells were treated with PBS. FL1-H and FL3-H indicate green color and red color intensities, respectively.

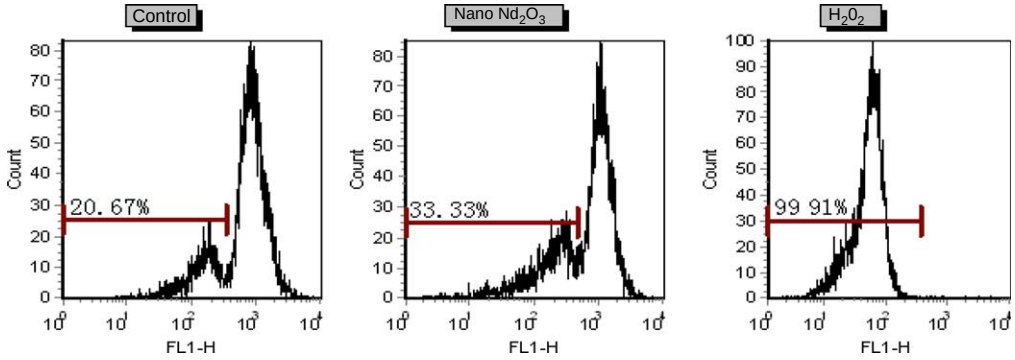

Fig. 5. Disruption of mitochondrial membrane potential in NCI-H460 cells by Nano Nd_2O_3. Mitochondrial membrane potential in cells treated with or without Nano Nd_2O_3 (45 μg/ml, 2 days) was measured by rhodamine 123 fluorescence using FACS. H_2O_2 (50 μM, 4 h) was used as a positive control.

cellular processes for cells to continually maintain proper protein levels and to respond to situations such as stress. In general, proteasome is responsible for degradation of short-lived proteins while autophagy for degradation of organelles and long-lived proteins. To assess the possible change in proteasome activity during Nano Nd_2O_3-induced autophagy, we assayed 20S proteasome activity in NCI-H460 cells by monitoring the release of free AMC from the fluorogenic peptide Suc-LLVY-AMC. As shown in Fig. 6, Nano Nd_2O_3 treatment (45 μg/ml, 2 days) caused a 41.48% decrease in proteasome activity, compared to the untreated cells.

Bafilomycin A1 but not 3-MA induced apoptosis while inhibiting autophagy

Recent studies have shown that bafilomycin A1 induced apoptosis while suppressing autophagy in a number of experimental cell systems. To assess whether bafilomycin A1 has a similar effect in Nano Nd_2O_3-treated cells, we stained NCI-H460 cells with Hoechst 33342 to detect apoptotic nuclei after treatment with Nano Nd_2O_3 (45 μg/ml) for 3 days. More than 400 cells were randomly selected and individually assessed under a microscope for the presence of apoptotic nuclei. Fig. 7A gives a represen-

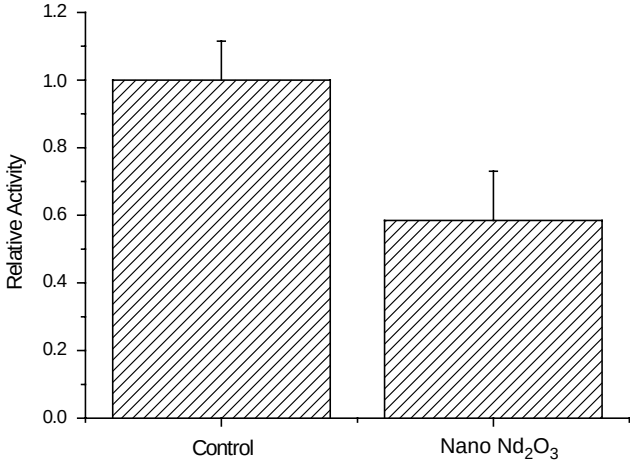

Fig. 6. Decrease of proteasome activity in Nano Nd_2O_3-treated NCI-H460 cells. Cells treated with or without Nano Nd_2O_3 (45 μg/ml, 2 days) were assayed for 20S proteasome activity as measured by release of the fluorescent group AMC from the fluorogenic substrate Suc-LLVY-AMC. Results were normalized against the control value. Means ± SD ($n = 4$). $p < 0.05$.

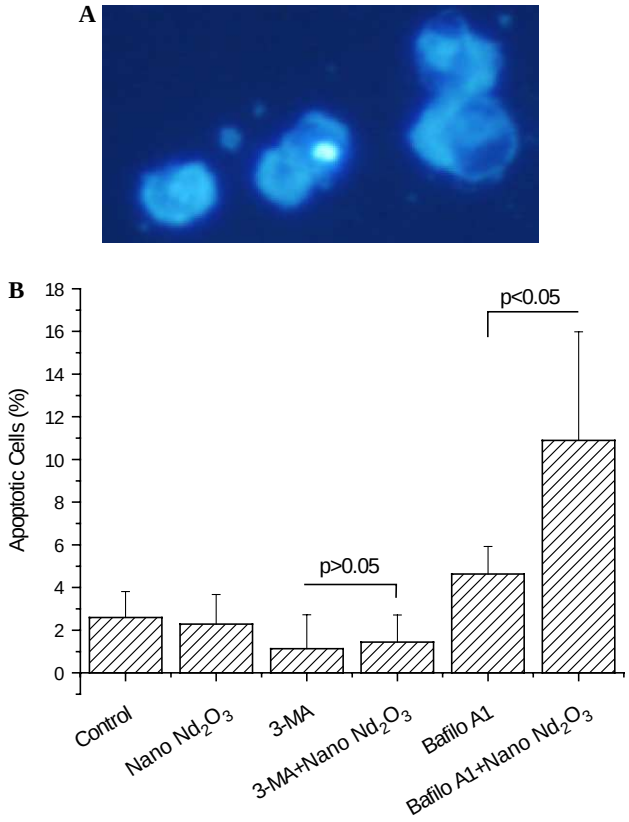

Fig. 7. Induction of apoptosis by bafilomycin A1/Nano Nd_2O_3 co-treatment in NCI-H460 cells. (A) Staining of apoptotic nuclei by Hoechst 33342. Fluorescent microscopy of representative apoptotic cells after co-treatment of Nano Nd_2O_3 (45 μg/ml) and bafilomycin A1 (20 nM) for 3 days. The bright fluorescence indicates condensation of DNA. (B) Quantification of apoptosis. Cells were treated with Nano Nd_2O_3 (45 μg/ml), bafilomycin A1 (20 nM) or 3-MA (2 mM). For combination treatments, cells were pre-treated with bafilomycin A1 (20 nM) or 3-MA (2 mM) for 1 h before treatment with Nano Nd_2O_3 (45 μg/ml). Control cells were treated with PBS. At least 150 cells from each sample were examined under a fluorescent microscope and the percentage of apoptotic cells was calculated. Means ± SD ($n = 3$).

tative picture of cell nuclei exhibiting features of DNA condensation. Co-treatment of NCI-H460 cells with bafilomycin A1, but not 3-MA, significantly increased the proportion of apoptotic cells from <3% to 11% (Fig. 7B). Treatment with bafilomycin A1 alone did not lead to this increase. These results indicated that bafilomycin A1, but not 3-MA, induced apoptosis while inhibiting autophagy caused by Nano Nd_2O_3.

Discussion

In this paper, we report for the first time that a rare earth compound, neodymium oxide, induces autophagic cell death in a cancer cell line. Neodymium is a lustrous, silver-yellow, rare-earth metallic element in the lanthanide series within group IIIb of the periodic table. Neodymium oxide, also called Neodymia, is widely used for making glass, capacitors, and magnets. The ability of neodymium oxide to induce autophagy is both element- and compound-specific, as neither neodymium chloride nor nano cerium oxide induced autophagy. Size appears to matter, as non-nano neodymium oxide was much less active than Nano Nd_2O_3 in inducing autophagy (data not shown).

We delineated that Nano Nd_2O_3 induced autophagy in NCI-H460 cells, while apoptosis and caspases were not involved. However, bafilomycin A1 induced apoptosis while inhibiting Nano Nd_2O_3-induced autophagy. These results suggested that there were crosstalks between apoptosis and autophagy, and inhibition of one pathway may drive cells to the other one [22]. It is conceivable that failure to remove disrupted mitochondria may prime cells for apoptosis. Alternatively, inhibition of autophagy may alter the equilibrium state between pro- and anti-apoptotic mediators [23] and drive cells to apoptosis.

Nano Nd_2O_3 also induced S-phase arrest in NCI-H460 cells. S-phase arrest during autophagy has been reported in several other cancer cell systems. Examples included prostate cancer cells treated with prostaglandin J2 [24], ovarian cancer cells treated with resveratrol [25], and colon cancer cells treated with soybean B-group triterpenoid saponins [26]. However, the relationship between S-phase arrest and autophagy, if any, remains to be determined.

Another important aspect emerging from our study is the finding that proteasome activity was greatly reduced during autophagy induced by Nano Nd_2O_3. Inhibition of the proteasome represents a new and promising approach for cancer therapy, with the clinical development of Bortezomib as a good example [27]. Inhibition of proteasome activity has been reported to occur during autophagy induced by mutant α-synuclein in PC12 cells [28]. It is interesting to note that α-synuclein is degraded by both proteasome and autophagy [29]. Whether the inhibition of proteasome activity by Nano Nd_2O_3 contributes to autophagy remains to be determined.

Nano Nd_2O_3 induced autophagic cell death in NCI-H460 cells in the micromolar equivalent concentration range, a range that is achievable clinically. Many chemotherapeutic compounds were known to work within this range. The physicochemical features of neodymium oxide, such as its magnetic property, may be useful for the development of innovative therapeutics for cancer. For example, it is conceivable that Nano Nd_2O_3, upon administration, could be concentrated in the cancerous organ or tissue by the use of a magnetic force, thus enhancing its therapeutic benefits while minimizing its toxicity. Similar "magnetic drug targeting" has been documented [30]. Nano Nd_2O_3 could also be conjugated with other chemotherapeutic drugs, such as drugs that induce apoptosis, leading to the possible development of more powerful therapeutics.

In conclusion, we demonstrated that Nano Nd_2O_3 induced massive vacuolization and autophagic cell death in NCI-H460 cells. Our results revealed a novel biological function for a nano-sized rare earth compound and point to new possibilities in developing innovative therapeutics for NLCSC and possibly other types of cancer.

Acknowledgments

We thank Prof. Yoshihide Tsujimoto (Osaka University, Japan) for providing 3-methyladenine. This work was supported by the One Hundred Talent Project of the Chinese Academy of Sciences, Anhui Talent Fund (2004Z023), and the National Natural Science Foundation of China (30470871).

References

[1] C.G. Ferreira, S.W. Span, G.J. Peters, F.A.E. Kruyt, G. Giaccone, Chemotherapy triggers apoptosis in a caspase-8-dependent and mitochondria-controlled manner in the non-small cell lung cancer cell line NCI-H460, Cancer Res. 60 (2000) 7133–7141.
[2] M. Fukuoka, S. Yano, G. Giaccone, T. Tamura, K. Nakagawa, J.-Y. Douillard, Y. Nishiwaki, J. Vansteenkiste, S. Kudoh, D. Rischin, R. Eek, T. Horai, K. Noda, I. Takata, E. Smit, S. Averbuch, A. Macleod, A. Feyereislova, R.-P. Dong, J. Baselga, Multi-institutional randomized phase II trial of gefitinib for previously treated patients with advanced non-small-cell lung cancer, J. Clin. Oncol. 21 (2003) 2237–2246.
[3] A. AS, S. Gultekin, E. Baehrecke, Autophagy in human tumors: cell survival or death? Cell Death Differ. 11 (2004) 1046–1048.
[4] E.H. Baehrecke, Autophagy: dual roles in life and death? Nat. Rev. Mol. Cell Biol. 6 (2005) 505.
[5] L.E. Broker, F.A.E. Kruyt, G. Giaccone, Cell death independent of caspases: a review, Clin. Cancer Res. 11 (2005) 3155–3162.
[6] D.J. Klionsky, Autophagy, Curr. Biol. 15 (2005) R282.
[7] X. Qu, J. Yu, G. Bhagat, N. Furuya, H. Hibshoosh, A. Troxel, J. Rosen, E.-L. Eskelinen, N. Mizushima, Y. Ohsumi, G. Cattoretti, B. Levine, Promotion of tumorigenesis by heterozygous disruption of the beclin 1 autophagy gene, J. Clin. Invest. 112 (2003) 1809–1820.
[8] C.K. Shunji Chi, K. Noguchi, T. Mochizuki, Y. Nagashima, M. Shirouzu, H. Fujita, M. Yoshida, W. Chen, A. Asai, M. Himeno, S. Yokoyama, Y. Kuchino, Oncogenic ras triggers cell suicide through the activation of a caspase-independent cell death program in human cancer cells, Oncogene 18 (1999) 2281–2290.
[9] S. Paglin, T. Hollister, T. Delohery, N. Hackett, M. McMahill, E. Sphicas, D. Domingo, J. Yahalom, A Novel response of cancer cells

to radiation involves autophagy and formation of acidic vesicles, Cancer Res. 61 (2001) 439–444.
[10] L.Z. Takao Kanzawa, L. Xiao, I.M. Germano, Y. Kondo, S. Kondo, Arsenic trioxide induces autophagic cell death in malignant glioma cells by upregulation of mitochondrial cell death protein BNIP3, Oncogene 24 (2005) 980–991.
[11] S. Daido, T. Kanzawa, A. Yamamoto, H. Takeuchi, Y. Kondo, S. Kondo, Pivotal role of the cell death factor BNIP3 in ceramide-induced autophagic cell death in malignant glioma cells, Cancer Res. 64 (2004) 4286–4293.
[12] G.I. Kanzawa, T. Komata, H. Ito, Y. Kondo, S. Kondo, Role of autophagy in temozolomide-induced cytotoxicity for malignant glioma cells, Cell Death Differ. 11 (2004) 448–457.
[13] I.F. Cristina Go'mez-Santos, A.F. Santidria'n, M. Barrachina, S.A. Joan Gil, Dopamine induces autophagic cell death and alpha-synuclein increase in human neuroblastoma SH-SY5Y cells, J. Neurosci. Res. 73 (2003) 341–350.
[14] A.D.-S. Pazit Tal-Or, Z. Lupowitz, R. Pinkas-Kramarski, Neuregulin promotes autophagic cell death of prostate cancer cells, Prostate 55 (2003) 147–157.
[15] Y. Shao, Z. Gao, P.A. Marks, X. Jiang, Apoptotic and autophagic cell death induced by histone deacetylase inhibitors, Proc. Natl. Acad. Sci. USA 101 (2004) 18030–18035.
[16] F.P. Lizon, Chemical toxicity of some actinides and lanthanides towards alveolar macrophages: an in vitro study, Int. J. Radiat. Biol. 75 (1999) 1459–1471.
[17] X.B. Ji, Z.H. Wang, M.Z. Cui, Y.Y. Lu, The suppression effect of light rare earth elements on proliferation of two cancer cell lines, Biomed. Environ. Sci. 13 (2000) 287–292.
[18] L.J. Dai, J. Li, L. Yu, G. Dai, A. Hu, L. Yuan, Z. Wen, Effects of rare earth compounds on growth and apoptosis of leukemic cell lines, In Vitro Cell Dev. Biol. Anim. 38 (2002) 373–375.
[19] F. Pajonk, J. Himmelsbach, K. Riess, A. Sommer, W.H. McBride, The Human immunodeficiency virus (HIV)-1 protease inhibitor saquinavir inhibits proteasome function and causes apoptosis and radiosensitization in non-HIV-associated human cancer cells, Cancer Res. 62 (2002) 5230–5235.
[20] F. Chen, L.E. Harrison, Ciglitazone-induced cellular anti-proliferation increases p27kip1 protein levels through both increased transcriptional activity and inhibition of proteasome degradation, Cell. Signal. 17 (2005) 809.
[21] Y.A. Saeki, E. Okuma, Y. Yazaki, S.A. Susin, G. Kroemer, F. Takaku, Bcl-2 down-regulation causes autophagy in a caspase-independent manner in human leukemic HL60 cells, Cell Death Differ. 7 (2000) 1263–1269.
[22] E.C. Piacentini, P.G. Mastroberardino, R. Nardacci, G. Kroemer, Does prothymosin act as molecular switch between apoptosis and autophagy? Cell Death Differ. 10 (2003) 937–939.
[23] P. Boya, R.-A. Gonzalez-Polo, N. Casares, J.-L. Perfettini, P. Dessen, N. Larochette, D. Metivier, D. Meley, S. Souquere, T. Yoshimori, G. Pierron, P. Codogno, G. Kroemer, Inhibition of macroautophagy triggers apoptosis, Mol. Cell. Biol. 25 (2005) 1025–1040.
[24] R. Butler, S.H. Mitchell, D.J. Tindall, C.Y.F. Young, Nonapoptotic cell death associated with S-phase arrest of prostate cancer cells via the peroxisome proliferator-activated receptor {gamma} ligand, 15-deoxy-{delta}12,14- prostaglandin J2, Cell Growth Differ. 11 (2000) 49–61.
[25] A.W. Opipari Jr., L. Tan, A.E. Boitano, D.R. Sorenson, A. Aurora, J.R. Liu, Resveratrol-induced autophagocytosis in ovarian cancer cells, Cancer Res. 64 (2004) 696–703.
[26] A.A. Ellington, M. Berhow, K.W. Singletary, Induction of macro-autophagy in human colon cancer cells by soybean B-group triterpenoid saponins, Carcinogenesis 26 (2005) 159–167.
[27] B.A. Teicher, G. Ara, R. Herbst, V.J. Palombella, J. Adams, The proteasome inhibitor PS-341 in cancer therapy, Clin. Cancer Res. 5 (1999) 2638–2645.
[28] L. Stefanis, K.E. Larsen, H.J. Rideout, D. Sulzer, L.A. Greene, Expression of a53t mutant but not wild-type alpha-synuclein in PC12 cells induces alterations of the ubiquitin-dependent degradation system, loss of dopamine release, and autophagic cell death, J. Neurosci. 21 (2001) 9549–9560.
[29] J.L. Webb, B. Ravikumar, J. Atkins, J.N. Skepper, D.C. Rubinsztein, {alpha}-Synuclein is degraded by both autophagy and the proteasome, J. Biol. Chem. 278 (2003) 25009–25013.
[30] C. Alexiou, W. Arnold, R.J. Klein, F.G. Parak, P. Hulin, C. Bergemann, W. Erhardt, S. Wagenpfeil, A.S. Lubbe, Locoregional cancer treatment with magnetic drug targeting, Cancer Res. 60 (2000) 6641–6648.